BMC Pediatrics

CASE REPORT

Open Access

Generalized lymphatic anomaly in a pediatric patient manifesting as a rare presentation of hemorrhagic pleural effusion: a case report

Xuehong Zhang[1], Jiuling Wang[1], Shouxing Duan[1], Yongping Yan[1] and Libin Wang[1*]

Abstract

Background Generalized lymphatic anomaly (GLA) is a rare congenital lymphatic malformation (LM) characterized by multiple infiltrating lymphangiomas in various tissues. Owing to its rarity, information on this disease is obtained mainly through case reports, leading to delayed diagnosis. In this study, we reported a case of generalized lymphatic anomaly in a pediatric patient manifesting as hemorrhagic pleural effusion.

Case presentation A 6-year-old female presented with abdominal pain, shortness of breath, chronic cough with yellow sputum production, and diminished respiration accompanied by pleural effusion. Imaging revealed significant left-sided pleural effusion with mediastinal involvement, left lung atelectasis, and multiple cystic lesions in both liver and spleen. Thoracoscopic exploration was conducted in response to her active intrathoracic bleeding, which identified a persistently hemorrhagic mass in the left mediastinum. The mass in the left mediastinum was removed, and pathological examination confirmed hyperplasia and expansion of the papillary endothelial cells within the lymphatic vessels. After intensive anti-infection therapy and symptomatic and supportive treatment, the patient's condition improved significantly. The regular outpatient follow-ups were continued until July 2024. Subsequent positron emission tomography (PET)CT at another hospital revealed multiple skeletal lesions in the limbs. Following treatment with sirolimus, no recurrence of pleural effusion was observed, and the patient's condition remained stable.

Conclusion In patients with generalized lymphatic anomalies (GLAs), involvement of the thoracic cavity may lead to hemorrhagic pleural effusion, thereby broadening the landscape of GLA phenotypic presentations. Furthermore, this case highlights the importance of complete radiological evaluation of susceptible patients with GLA to avoid diagnostic delay in this morbid condition. We also review recently discovered genetic changes underlying lymphatic anomaly development and the progress of treatment.

Keywords Child, Generalized lymphatic anomalies, Lymphatic malformations, Lymphangioma

*Correspondence:
Libin Wang
wanglibin007@126.com
[1]Department of Pediatrics, Huazhong University of Science and Technology Union Shenzhen Hospital, Shenzhen, China

Background

Generalized lymphatic anomalies (GLAs) are rare multiorgan congenital disorders that arise from the abnormal proliferation of lymphatic vessels, resulting in abnormally dilated connected thin-walled lymphatic channels. GLAs can frequently occur in the thoracic and abdominal regions, affecting multiple organs, with the most common being the lungs and bones [1]. This condition predominantly affects children and young adults in the first two decades of life [2]. The diagnosis of GLA is often delayed due to its rarity and diverse clinical presentations. To date, there are no standard treatment guidelines for GLA, and the treatment for GLA is mostly supportive [3]. Here, we analysed and reported a case of GLA in a 6-year-old female manifesting as uncommon hemorrhagic pleural effusion, which may enhance our understanding of the clinical heterogeneity associated with GLA and highlight lymphatic malformations as a rare cause of hemorrhagic pleural effusion.

Case presentation

Patient presentation

On June 26, 2023, a 6-year-old female patient was admitted to our hospital, presenting with abdominal pain for two months, a cough for one month, and pleural effusion that had emerged one day prior to admission. Two months prior to admission, the child experienced intermittent abdominal pain without any clear cause. Accompanied by poor appetite and nausea, the patient's condition was not dramatic and could be relieved, so she underwent no special treatment. She experienced a nocturnal cough accompanied by yellow sputum for one month. In addition, she experienced a daily fever peaking at 38.0℃. She was found to have pleural effusion incidentally during an abdominal ultrasound examination at another hospital and was thus referred to our hospital. The patient had no contributing past medical history.

Physical examination

Upon physical examination, her body temperature was 38 °C. Her respiratory rate and heart rate were moderately accelerated. Respiratory sounds in the left superior pulmonary were weakened and disappeared in the left middle and lower lungs. Several lymph nodes with a diameter of 1 cm were found in the neck, without tenderness or adhesion.

Laboratory findings

Laboratory examinations revealed that the white blood cell count was 4.1×10^9/L, the red blood cell count was 4.38×10^{12}/L, the haemoglobin concentration was 92 g/L, the platelet count was 335×10^9/L, the neutrophil percentage was 57.6%, the lymphocyte percentage was 32.2%, the monocyte percentage was 8.2%, and the C-reactive protein concentration was 2.95 mg/L. The procalcitonin concentration was 0.4 ng/ml, and the erythrocyte sedimentation rate was 6 mm/h. The results of the pleural effusion routine revealed that the colour was red and cloudy, the total number of red blood cells was 2.51×10^6/L, the pH was 7.2, the total number of white blood cells was 1.76×10^6/L, the carcinoembryonic antigen (CEA) concentration was 0.77 ng/ml, the GLU concentration was 3.4 mmol/L, the lactate dehydrogenase (LDH) concentration was 238 U/L, and the adenosine deaminase (ADA) concentration was 7.1 U/L. No significant abnormalities were observed in coagulation function, liver function, kidney function, thyroid function, the antinuclear antibody spectrum, or routine urine and stool analyses. Aetiological detection included multiple respiratory pathogenic antibodies (IgM), pleural effusion smear, tuberculosis-infected T-cell detection, acid–fast bacillus tests, and high-throughput metagenomic sequencing technology to detect pathogenic microorganisms. There was no obvious abnormality.

Imaging data

A plain thoracic CT scan (mediastinal window) revealed significant fluid accumulation in the left thoracic cavity, accompanied by a prominent hypodense area anterior to the cardiothoracic region (Fig. 1A, indicated by arrows). The adjacent lung tissue exhibited substantial compression, resulting in posterior displacement of both the heart and the thymus. The abdominal CT scan revealed multiple cystic lesions in the spleen and a rounded hypoechoic lesion in the liver (Fig. 1B). Abdominal ultrasonography revealed that the diameter and shape of the sections of the liver and spleen were normal and that the envelope was smooth. There was a circular echoless section with a clear boundary in the S7 section of the right lobe of the liver and multiple cystic dark areas in the spleen.

The patient exhibited hemorrhagic pleural effusion, as shown in Fig. 2. After several therapeutic aspirations of the pleural fluid, enhanced chest CT and enhanced abdominal CT were conducted. The results are as follows: a discernible decrease in pleural effusion within the left thoracic cavity; the presence of multiple enlarged lymph nodes along the thoracic aorta; a soft tissue mass shadow within the mediastinum; and various cystic lesions in the liver and spleen, as depicted in Fig. 3.

Pathological examination

To evaluate the characteristics of the mediastinum mass and hemorrhagic pleural effusion, and left thoracoscopic exploration was performed under general anaesthesia on June 29, 2023. A substantial volume of hemorrhage was observed in the left pleural cavity. A 4 cm×3 cm tumor was observed in the left lower lung root. The tumor had a broad base, and the boundary was not clear. After the

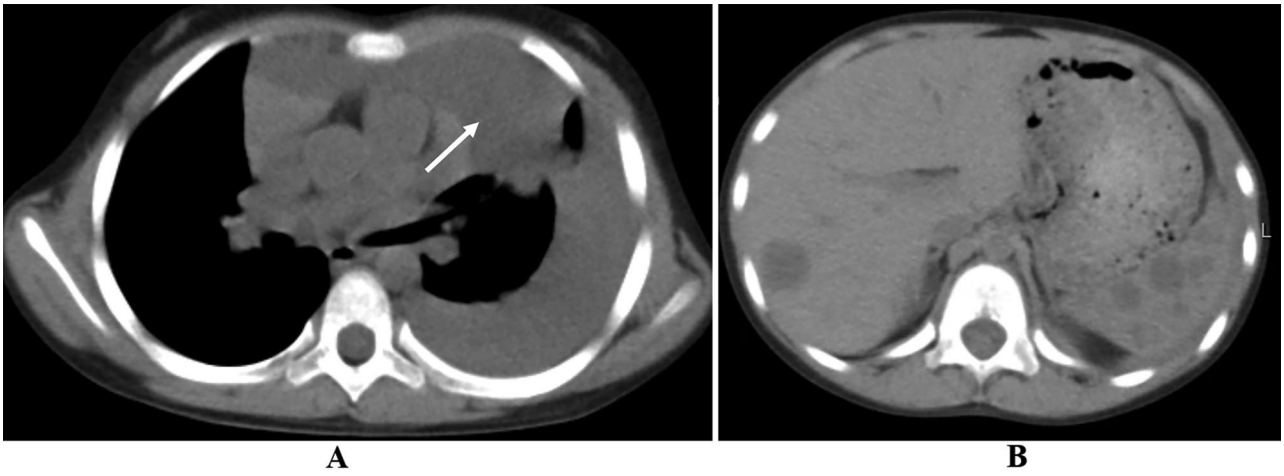

Fig. 1 Imaging findings of plain chest and abdomen CT scans prior to treatment. (**A**) Thoracic CT scan (mediastinal window) revealed extensive fluid accumulation in the left thoracic cavity, along with a conspicuous hypodense area anterior to the cardiothoracic region (indicated by arrows). The surrounding lung tissue exhibited marked compression, and both the heart and the thymus were pushed posteriorly due to compression. (**B**) An abdominal CT scan revealed multiple cystic lesions in the liver and spleen

Fig. 2 The pleural effusion was hemorrhagic, which was observed by clamping the drainage tube

tumor was removed from the base margin, there was no obvious active bleeding. The procedure was successful, the volume of intraoperative bleeding was 100 ml, and 2 units of red blood cells were transfused during the operation. The tumor was sent for histopathological examination. Microscopic observation revealed vascular hyperplasia in the fibrous adipocytes, and irregular fissure structures could be observed. Flaky distributed cells were observed within the lumen. Papillary endothelial cell proliferation was detected. A small amount of thymus tissue exhibited a nodular distribution. The immunohistochemical analysis demonstrated positivity for CD31, CD34, D2-40, ERG, and Ki67 (20%+) and negativity for CD68, HMB, CD45, Melan A, and S100. Collectively, these findings supported the diagnosis of lymphangioma (Fig. 4).

Diagnosis, treatment, and follow-Up

Considering the patient's medical history, thoracic and abdominal imaging results and pathological findings, the child was diagnosed with GLA. Following her admission to our hospital, relevant examinations were conducted to exclude any contraindications, after which she underwent closed thoracic drainage and intravenous antimicrobial therapy consisting of an azithromycin suspension, cefoperazone sodium and sulbactam sodium. A significant volume of dark red pleural effusion was evacuated. Following mediastinal tumor resection, the patient underwent closed thoracic drainage to facilitate the removal of pleural effusion. Furthermore, postoperatively, she underwent hemostasis, antiinfection, prevention of lung infection, promotion of lung re-expansion, and oil-free and low-fat diet and albumin infusion treatment to correct the symptoms of hypoalbuminemia. Regular routine examinations were performed, and blood tests revealed that haemoglobin levels were normal. Nine days after surgery, the pleural effusion turned light yellow, and there was a significant reduction in drainage flow. Eleven days after mediastinal tumor resection, the plain chest CT scan improved to evaluate the patient's condition, and the imaging findings revealed that the left pleural effusion had decreased compared with that in previous assessments. The lesions of the thoracic para-aortic lymph

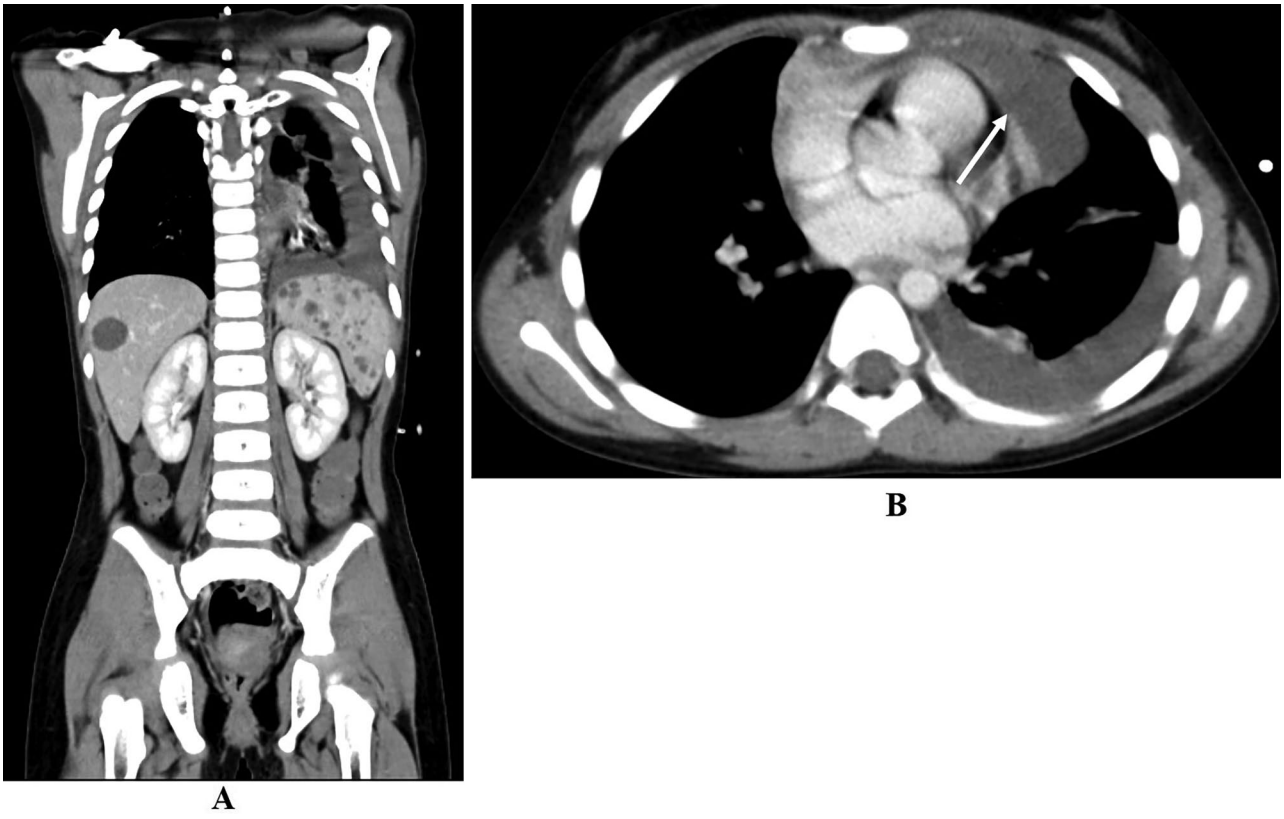

Fig. 3 Enhanced CT imaging findings of the chest and abdomen after closed thoracic drainage with partial pleural effusion. (**A**) Contrast-enhanced CT coronal reconstruction revealed that the left pleural effusion was slightly reduced, and the left lung exhibited atelectasis; multiple cystic lesions in the liver and spleen with clear margins and thin cyst walls and no obvious enhancement in contrast-enhanced scanning. (**B**) Contrast-enhanced CT of the transverse section of the chest revealed substantial fluid collection in the mediastinum that demonstrated no enhancement (indicated by arrows)

nodes, liver and spleen remained largely unchanged (Fig. 5). The surgical site exhibited satisfactory healing, and the drainage tube was removed on postoperative day 12. She was discharged 17 days after surgery. Following discharge, she underwent positron emission tomography (PET)CT at another hospital. PET-CT revealed multiple skeletal lesions in the limbs. She was treated with sirolimus to suppress the immune response, and the child's condition was continuously followed up and observed. Regular outpatient follow-ups were performed until July 2024. Routine chest ultrasonography revealed a small amount of pleural effusion with a depth of approximately 22 mm, which was not significantly greater than the measurements taken prior to discharge. The child's condition remained stable, and she had a normal diet, and no cough, anhelation, chest tightness, or other discomfort.

Discussion and conclusions

In 2018, ISSVA published a classification for vascular anomalies. Based on this classification, the group of lymphatic anomalies can be identified into common cystic LMs, GLAs, LMs in Gorham-Stout disease, channel-type LMs, primary lymphedema and acquired progressive lymphatic anomalies [3]. GLA, previously known as lymphangiomatosis, is characterized by the abnormal proliferation of lymphatic vessels, resulting in abnormally dilated, thin-walled lymphatic channels. These channels may be localized or commonly generalized, affecting multiple organ systems, with the lungs and bones being the most frequently involved [2]. Rodenberger first named this disease generalized cystic lymphangiomatosis in 1828 [4]. It usually occurs in childhood or early adulthood. Earlier disease is generally more aggressive, which can lead to a higher mortality rate as patients die from multiorgan failure [2]. In this case, multiple organs and tissues, including the mediastinum, lung root, liver and spleen were affected, thereby confirming the diagnosis of GLA.

At present, the exact pathogenesis of GLA is still unclear. A variety of genes and regulatory factors may be involved in the regulation of lymphangiogenesis and promote abnormal dilatation of the lumen, which leads to the occurrence of LM in children. Recent studies have linked GLA to somatic mutations in the *PIK3CA* gene [5, 6]. With whole-exome sequencing, Wang et al. identified new pathogenic genes in LM patients, namely, somatic *mutations of PIK3CA (c.1633G > A [p.E545K])* and *PIK3CD (c.1997T > C [p.L666P])* [7]. The pathogenicity of

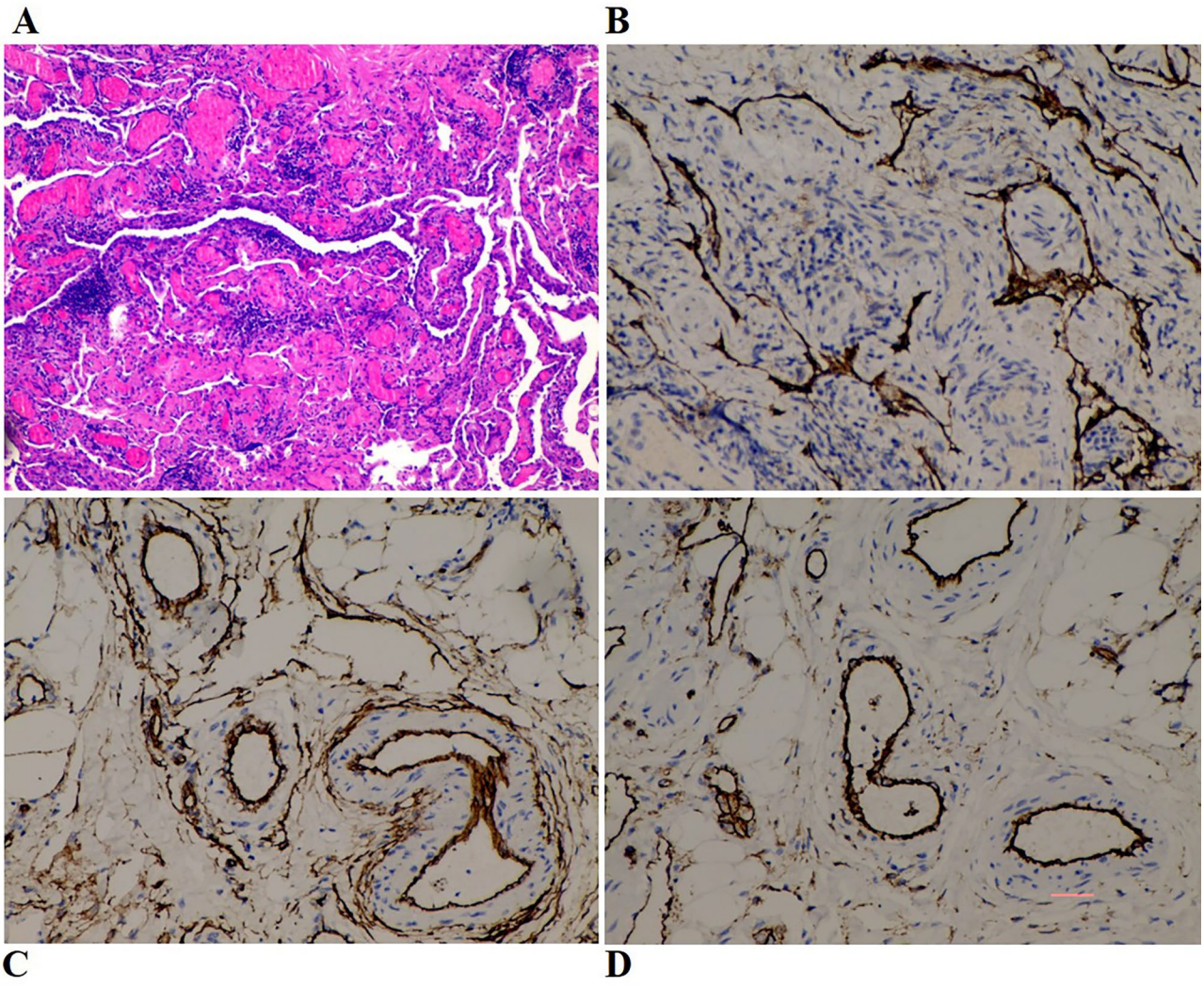

Fig. 4 Pathological results of the patient. **A** HE staining (×100); **B** Immunostaining for D2-40 is positive (×200); **C** Immunostaining for CD34 is positive (×200); **D** Immunostaining for CD31 is positive (×200)

the novel mutation *c.1997T > C* in *PIK3CD* was identified through an in vitro functional study, which suggested that downstream signalling in endothelial cells can be affected by *PIK3CD* mutations. *PIK3CD* can disrupt normal lymphangiogenesis and contribute to LM development. Vascular endothelial growth factor (VEGF) is an important molecule that regulates lymphangiogenesis. Lymphangiogenesis is driven mainly by VEGF-C and the lymph-specific receptor VEGFR-3, but also by VEGF-A [8]. Ozeki et al. reported that serum VEGF levels increased significantly in patients with diffuse pulmonary lymphangiomatosis (DPL) and decreased significantly with the remission of the disease [9]. Alternatively, abnormal activation of tyrosine kinase (PTK) may be involved in the pathogenesis of GLA. Tyrosine kinase (PTK) inhibitors have been investigated in multiple case reports [10, 11].

GLA is characterized by the absence of specific clinical manifestations and may affect a single organ system or multiple organ systems other than the brain. Potential presentations include thoracic lesions (including pleural effusion, chylothorax, and mediastinal cystic lesions), abdominal pathologies (such as ascites, splenic cysts, and retroperitoneal cystic lesions), osseous resorption lesions (affecting the skull, ribs, pelvis, and spine), and dermatological anomalies (including lymphedema and lymphatic leakage) [12]. Approximately 75% of children with GLA have skeletal involvement, which can manifest as bone pain and pathological fracture [13]. The GLA affects all the skeleton, which commonly involves the ribs, skull vault, and extremity long bones. These lesions rarely resolve spontaneously and usually lead to severe bone pain, pathological fractures, and joint deformities due to extreme osteolysis [14]. Literature elucidating the skeletal pathological manifestations is rare. Pleural effusions are often chylous due to spontaneous rupture of diseased lymph vessels within the lymphangiomas [15].

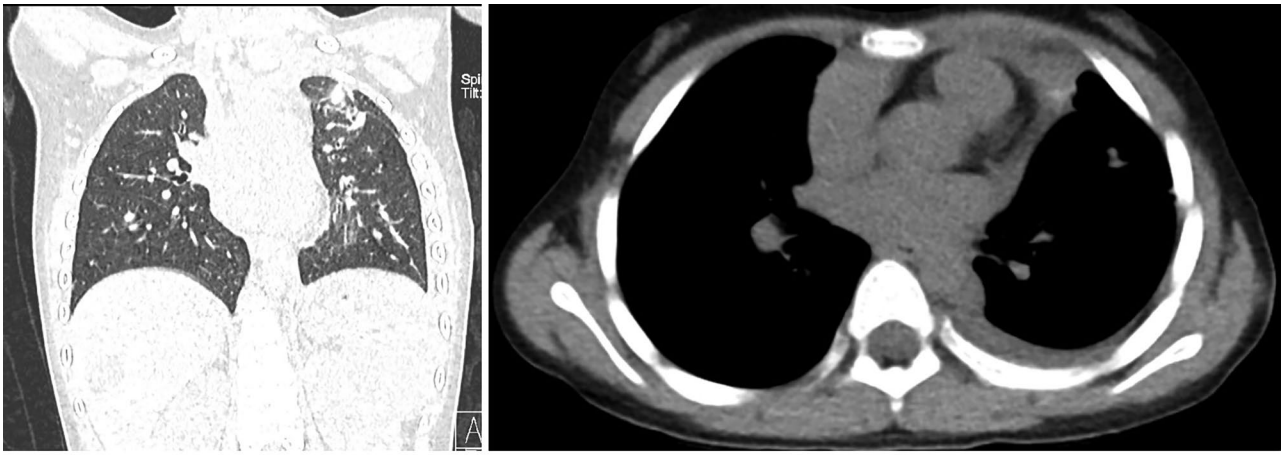

Fig. 5 Coronal plain CT scan postresection of the mediastinal mass. **A** plain coronal CT scan revealed a marked reduction in left pleural effusion compared with the previous scan, with expanded compressed lung tissue. **B** CT scan of the mediastinal window revealed that the large anterior hypodensity in the heart region had resolved

Ayşe Keven et al. reported that the median age of the sample was 9 years at admission (min. 3, max. 12) in a retrospective study consisting of six pediatric patients diagnosed with GLA. The most common clinical symptom of GLA patients at admission was dyspnea, usually accompanied by pleural effusion, which was chylous in all patients. Bone involvement was the most prevalent extrathoracic finding, while abdominal involvement was primarily asymptomatic, with the spleen being the organ most frequently affected in this region [16]. Pablo Ramallo et al. presented a case involving a 14-year-old male patient diagnosed with GLA who primarily presented with symptoms of asthenia, low back pain, and abdominal distension. Ascites and numerous small splenic and rare pancreatic cystic lesions are found in the abdomen [12], which further implies that patients with GLA may develop cystic lesions in any organ possessing lymphatic channels. The proliferation of lymphangiomas only within the thorax leads to the rare syndrome of DPL. DPL usually involves both lungs, the mediastinum, the pleura, and other thoracic organs but has no extrathoracic lymphatic involvement. Patients with DPL usually have an insidious onset, and the younger the age of onset is, the worse the prognosis [17]. Patients with DPL typically present with symptoms such as cough, chest tightness, sputum production, dyspnea, and shortness of breath. Additionally, some patients may exhibit recurrent intractable chylothorax, anemia and disseminated intravascular coagulation (DIC) [18].

In this case, the patient primarily presented with mild cough, abdominal pain, pleural effusion, and involvement of the liver, spleen, and bones, which is consistent with the literature. Importantly, this patient's pleural effusion was hemorrhagic and accompanied by active intrapleural hemorrhage; nevertheless, similar reports are rare. The sustained presence of hemothorax markedly impacts subsequent diagnostic and therapeutic strategies. Conversely, whether hemorrhagic pleural effusion portends a worse prognosis requires further clinical investigation for validation.

The diagnosis of GLA is usually delayed because patients often present with unrelated symptoms, such as fragility fractures, and GLA may be discovered incidentally. Biopsy is necessary for the diagnosis of GLA. The following histochemical methods are recommended: hematoxylin and eosin staining, CD31 (panendothelial cell marker), podoplanin (lymphatic endothelial marker recognized by the D2-40 antibody), and CD34 (blood endothelial marker occasionally expressed by lymphatics) [19]. Nevertheless, GLA often involves multiple systems, and obtaining biopsy samples from multiple affected organs and tissues at the same time is difficult and may not be accepted by parents. Therefore, limb bones and superficial soft tissues can be selected as biopsy sites [20].

CT is valuable in the diagnosis of lymphangiomatosis and can improve the coincidence rate of the initial diagnosis of the disease. CT imaging typically reveals well-defined cystic masses across various organ systems. Multiple dilated cystic lesions are observed in multiple bones, with a soap bubble-like appearance, clear boundaries, and uniform low density [21]. Whole-body CT is thought to be important for evaluating the extent of organ involvement, and CT manifestations may present as well-demarcated osteolytic bone lesions with a sclerotic margin, which can affect multiple bones in proximity [22]. These characteristics were also corroborated by our case, with the involvement of limb bones and multiple organ systems. In addition, advanced magnetic

resonance imaging (MRI) is typically used to evaluate the extent of a lesion if it is atypical, large, or deep in location due to its nonradiation, multidirectional imaging and especially high sensitivity to liquid components. MRI can also provide effective imaging evidence for diagnosis and plays a crucial role in posttreatment follow-up, particularly in cases involving large or complex LMs [23, 24]. In recent years, lymphatic scintigraphy and single-photon emission computerized tomography (SPECT), which can detect and evaluate some rare lymphatic diseases, have also been applied in the diagnosis of LM. Indocyanine green (ICG) contrast agent is a near-infrared fluorescent contrast agent with low toxicity in biological tissues and good penetration ability. Currently, it is gradually being applied to the diagnosis and treatment of lymphatic diseases.

Since the imaging features, clinical findings and complications of GLA often overlap with those of kaposiform lymphangiomatosis (KLA) and Gorham-Stout disease (GSD), many authors have grouped them into complex lymphatic anomalies (CLAs) [12]. Nevertheless, certain features allow us to distinguish one from the other. According to the latest edition of the ISSVA guidelines, KLA has been classified as a subtype of generalized lymphatic anomaly (GLA) [3]. In KLA, there are multiple noncontiguous, lytic, and cortex-sparing lesions. This condition can manifest as severe coagulation disorder and hemorrhagic pericardial and pleural effusion due to a low platelet count (50000–100000/μL) [12]. While Gorham-Stout disease, also known as vanishing bone disease, shares similarities with GLA and KLA, it is a distinct pathological entity characterized by progressive osteolysis leading to destruction of the cortical bone and heightened osteoclast activity. In contrast, the GLA and KLA present with osteolytic lesions localized within the medullary cavity while preserving the integrity of the cortical bone [12].

In our patient, early thoracoscopic exploration and pathological examination were imperative because of persistent massive hemorrhagic pleural effusion. During the thoracoscopic procedure, it was observed that the mediastinal tumor exhibited a multilocular cystic morphology and presented with continuous bleeding. After the pleural effusion was drained, resection of the mass was conducted, and tissue samples were sent for pathological examination, which confirmed that the mass was a lymphatic malformation. A limitation of our study was the lack of a comprehensive evaluation of skeletal lesions when considering the diagnosis of GLA; subsequently, during follow-up at another institution, skeletal lesions in the limbs were identified following a PET–CT scan. These findings suggest that systemic imaging evaluation is essential for a thorough assessment of the GLA. This patient had osteolytic lesions within the medullary cavity with cortical bone sparing, findings that enabled us to exclude this diagnosis of GSD.

There are currently no standard treatment options or treatment guidelines for GLA. The main therapeutic goals are to delay disease progression, actively treat complications, and relieve symptoms [20]. A variety of medical treatment modalities have been proposed, including interferon therapy, immunosuppression, immunotherapy and chemotherapy [5, 11, 25]. Treatment with surgery, laser therapy or radiotherapy may be used for symptomatic solitary lesions. However, for diffuse lesions, it is almost impossible to completely remove the lesion tissue through surgery, and it is easy to relapse after surgery. Therefore, a combination of multiple methods can be used to treat LM cases that are difficult to control with a single method. Alternatively, observation alone is reasonable for asymptomatic solitary lesions [20]. As an inhibitor of the mTOR pathway, sirolimus can inhibit abnormal activation of the *PI3K-AKT-mTOR* pathway, thereby inhibiting abnormal proliferation of blood vessels. Sirolimus is currently the most widely used oral drug and is widely used for refractory lymphatic and vascular malformations. Many clinical studies and case reports have shown that sirolimus is effective in the treatment of most patients with GLA/DPL [5, 11, 26]. At present, there are many case reports concerning the application of tyrosine kinase inhibitors. Rossler et al. used sunitinib and paclitaxel to treat a GLA patient with respiratory failure and a GSD patient with back pain and swelling, and the results showed that sunitinib could improve the clinical and imaging manifestations of patients [27]. Interferon-α (IFN-α) has been reported as a potential therapeutic option in various cases, and its mechanism may involve the downregulation of vascular endothelial growth factor (VEGF) expression [28]. In recent years, with the application of bevacizumab and the emergence of new targeted drugs, IFN-α has been gradually replaced. In 2012, Aman et al. first reported the successful treatment of DPL with bevacizumab, a monoclonal anti-VEGF antibody, which resulted in a fast reduction in tumor size and immediate clinical improvement [29].

In this case, the intrathoracic lesions of the child were relatively independent. The active bleeding may have led to tracheal compression; therefore, surgical resection was adopted for treatment. The liver and spleen lesions were observed and followed up for asymptomatic reasons. With subsequent follow-up, she was treated with sirolimus, and her clinical status improved.

In summary, GLA is a rare and morbid disease in children. The diagnosis of GLA poses significant challenges due to its rarity and the overlap of clinical and radiological findings. Therefore, radiological imaging is crucial for early diagnostic confirmation. Bony lesions in the GLA can be radiologically differentiated from other complex

lymphatic diseases of bone, such as GSD and KLA. Moreover, it is essential to acknowledge that lymphatic malformations constitute a rare etiology of hemorrhagic pleural effusion. There is no standard treatment for GLA, and further study should be performed to fully understand its pathophysiological mechanisms and optimal treatment options, as well as to draft clinical management strategies for LMs (including LM, GLA, and GSD) to identify information on not only their etiology but also their specific management, long-term outcomes, and disease sequelae.

Abbreviations

GLA	Generalized lymphatic anomaly
ISSVA	International Society for the Study of Vascular Anomalies
CT	Chest computed tomography
CEA	Carcinoembryonic antigen
LDH	Lactate dehydrogenase
LM	Lymphatic malformation
ADA	Adenosine deaminase
DPL	Diffuse pulmonary lymphangiomatosis
DIC	Disseminated intravascular coagulation
MRI	Magnetic resonance imaging
SPECT	Single-photon emission computerized tomography
ICG	Indocyanine green
IFN-α	Interferon-α
VEGF	Vascular endothelial growth factor

Acknowledgements
We would like to thank the patient and her parents for their support in this study.

Author contributions
L.W guided the writing of the manuscript and edited the manuscript; X.Z and J.W collected the material and wrote the main manuscript text. X.Y and S.D prepared all the figures. All authors reviewed the manuscript and approved the submitted version.

Funding
No funding.

Data availability
The raw datasets generated and analyzed during the current study are not publicly available in order to protect participant confidentiality. The datasets obtained during the current study are available from the corresponding author if the requirements are reasonable.

Declarations

Ethical approval
This study was approved by the Ethics Committee of Huazhong University of Science and Technology Union Shenzhen Hospital (approval number: NO. LW-2024-032). All study procedures were conducted in accordance with the tenets of the Declaration of Helsinki. The patient and her parents provided written informed consent to participate in this study.

Consent for publication
Written informed consent to publish this case was obtained from the patient and her parents, including case descriptions and medical data.

Competing interests
The authors declare no competing interests.

Received: 1 March 2024 / Accepted: 20 December 2024
Published online: 06 January 2025

References

1. Snyder EJ, Sarma A, Borst AJ, Tekes A. Lymphatic anomalies in children: update on imaging diagnosis, Genetics, and treatment. AJR Am J Roentgenol. 2022;218(6):1089–101.
2. Alvarez OA, Kjellin I, Zuppan CW. Thoracic lymphangiomatosis in a child. J Pediatr Hematol Oncol. 2004;26(2):136–41.
3. Ozeki M, Fukao T. Generalized lymphatic anomaly and Gorham-Stout Disease: overview and recent insights. Adv Wound Care (New Rochelle). 2019;8(6):230–45.
4. Ozel A, Uysal E, Dokucu AI, Erturk SM, Basak M, Cantisani V. US, CT and MRI findings in a case of diffuse lymphangiomatosis and cystic hygroma. J Ultrasound. 2008;11(1):22–5.
5. Ricci KW, Hammill AM, Mobberley-Schuman P, Nelson SC, Blatt J, Bender JLG, McCuaig CC, Synakiewicz A, Frieden IJ, Adams DM. Efficacy of systemic sirolimus in the treatment of generalized lymphatic anomaly and Gorham-Stout disease. Pediatr Blood Cancer. 2019;66(5):e27614.
6. Dvorakova V, Rea D, O'Regan GM, Irvine AD. Generalized lymphatic anomaly successfully treated with long-term, low-dose sirolimus. Pediatr Dermatol. 2018;35(4):533–4.
7. Wang S, Wang W, Zhang X, Gui J, Zhang J, Guo Y, Liu Y, Han L, Liu Q, Li Y, Sun N, Liu Z, Du J, Tai J, Ni X. A somatic mutation in PIK3CD unravels a novel candidate gene for lymphatic malformation. Orphanet J Rare Dis. 2021;16(1):321. https://doi.org/10.1186/s13023-021-01946-7.
8. Wuest TR, Carr DJ. VEGF-A expression by HSV-1-infected cells drives corneal lymphangiogenesis. J Exp Med. 2010;207(1):101–15.
9. Ozeki M, Fukao T, Kondo N. Propranolol for intractable diffuse lymphangiomatosis. N Engl J Med. 2011;Apr7(14):1380–2.
10. Libby LJ, Narula N, Fernandes H, Gruden JF, Wolf DJ, Libby DM. Imatinib treatment of lymphangiomatosis (generalized lymphatic anomaly). J Natl Compr Cancer Netw. 2016 Apr;14(4):383–6.
11. Gurskytė V, Zeleckienė I, Maskoliūnaitė V, Mickys U, Šileikienė V. Successful treatment of diffuse pulmonary lymphangiomatosis with sirolimus. Respir Med Case Rep. 2020 Feb;1:29:101014.
12. Ramallo P, Blanque S, Méndez Uriburu L, Ahualli J, Méndez A, Méndez M. Case 311: generalized lymphatic anomaly. Radiology. 2023;306(3):e213229.
13. Wuest TR, Carr DJ. VEGF-A expression by HSV-1-infected cells drives corneal lymphangiogenesis. J Exp Med 2010 Jan 18;207(1):101–15.
14. Trenor CC 3rd, Chaudry G. Complex lymphatic anomalies. Semin Pediatr Surg. 2014;23(4):186–90.
15. Uhlenbruch M, Keymel S, Krüger S. Lymphangiomatose – seltene Ursache eines pleuraergusses [Lymphangiomatosis: Rare cause of Pleural Effusion]. Pneumologie. 2021;75(2):138–41. German.
16. Faul JL, Berry GJ, Colby TV, Ruoss SJ, Walter MB, Rosen GD, Raffin TA. Thoracic lymphangiomas, lymphangiectasis, lymphangiomatosis, and lymphatic dysplasia syndrome. Am J Respir Crit Care Med. 2000 Mar;161(3 Pt 1):1037–46.
17. Faul JL, Berry GJ, Colby TV, Ruoss SJ, Walter MB, Rosen GD, Raffin TA. Thoracic lymphangiomas, lymphangiectasis, lymphangiomatosis, and lymphatic dysplasia syndrome. Am J Respir Crit Care Med. 2000;161(3 Pt 1):1037–46.
18. Sun X, Lu C, Huang Z, Xu J, Zhu H, Yang S, Chen D. Diagnosis and treatment of diffuse pulmonary lymphangioma in children: a case report. Exp Ther Med. 2023;25(4):175.
19. Iacobas I, Adams DM, Pimpalwar S, Phung T, Blei F, Burrows P, Lopez-Gutierrez JC, Levine MA. Trenor CC 3rd. Multidisciplinary guidelines for initial evaluation of complicated lymphatic anomalies-expert opinion consensus. Pediatr Blood Cancer. 2020;67(1):e28036.
20. Liu T, Basseri S, Mussari B, et al. Generalized lymphatic anomalies and review of the current management landscape: a case report and review of the literature. J Med Case Rep. 2021;15(1):398.
21. Ding C, Wang Y, Radiographic. CT, and MRI features of generalized lymphatic anomaly in a boy. Curr Med Imaging. 2023;19(2):194–8.
22. Kwag E, Shim SS, Kim Y, Chang JH, Kim KC. CT features of generalized lymphangiomatosis in adult patients. Clin Imaging. 2013 Jul-Aug;37(4):723–7.
23. De Leacy R, Bageac DV, Manna S, Gershon BS, Kirke D, Shigematsu T, Sinclair C, Chada D, Som P, Doshi A, Nael K, Berenstein A. A radiologic grading system for assessing the radiographic outcome of treatment in lymphatic and lymphatic-venous malformations of the head and neck. AJNR Am J Neuroradiol. 2021;42(10):1859–64.
24. Durand R, Reid JR, Belasco JB, Shellikeri S, Calle-Toro JS, Cahill AM, Srinivasan A. MRI for response assessment of extensive lymphatic malformations in children treated with sirolimus. AJR. 2021;217:741–52.

25. Onyeforo E, Barnett A, Zagami D, Deller D, Feather I. Diffuse pulmonary lymphangiomatosis treated with bevacizumab. Respirol Case Rep 2018 Nov 28;7(1): e00384.
26. Dvorakova V, Rea D, O'Regan GM, Irvine AD. Generalized lymphatic anomaly successfully treated with long-term, low-dose sirolimus. Pediatr Dermatol 2018 Jul;35(4):533–4.
27. Rössler J, Saueressig U, Kayser G, von Winterfeld M, Klement GL. Personalized therapy for generalized lymphatic anomaly/Gorham–Stout disease with a combination of sunitinib and taxol. J Pediatr Hematol/Oncol. 2015 Nov;37(8):e481–5.
28. Timke C, Krause MF, Oppermann HC, Leuschner I, Claviez A. Interferon alpha 2b treatment in an eleven-year-old boy with disseminated lymphangiomatosis. Pediatr Blood Cancer. 2007 Jan;48(1):108–11.
29. Aman J, Thunnissen E, Paul MA, van Nieuw Amerongen GP, Vonk-Noordegraaf A. Successful treatment of diffuse pulmonary lymphangiomatosis with bevacizumab. Ann Intern Med. 2012 Jun;5(11):839–40.

Publisher's note